Myosin S1 Changes the Orientation of Caldesmon on Actin†

Danuta Szczesna,‡ Philip Graceffa, C.-L. Albert Wang, and Sherwin S. Lehrer*

Boston Biomedical Research Institute, 20 Staniford Street, Boston, Massachusetts 02114

Received January 28, 1994; Revised Manuscript Received March 28, 1994®

ABSTRACT: Changes in the orientation of caldesmon bound to actin in skeletal ghost myofibrils caused by the binding of myosin subfragment 1 (S1) were measured by fluorescence-detected linear dichroism using fluorescence microscopy. Gizzard caldesmon, labeled with acrylodan at its two Cys residues (CaD*), bound to actin with a probe angle that was unaffected by actin-bound tropomyosin. Irrigation of fibrils with myosin S1 dissociated most of the bound CaD*, but reintroduction of CaD* resulted in its rebinding to actin, without dissociation of S1, with a 7° difference in probe angle. A similar change in probe angle was also observed when a 27-kDa actin-binding C-terminal fragment of caldesmon, labeled with acrylodan at its single Cys 580 (CaD-27*), was used. Introducing MgADP, which bound to S1 in the CaD*–actin–S1 ternary complex in the fibril, reversed the bound CaD* dichroism. These results indicate that (i) myosin heads and caldesmon compete for a common actin binding site; (ii) a ternary complex of CaD*–actin–S1 can be formed with an orientation of CaD* different from that in the CaD*–actin binary complex, and (iii) MgADP, which binds to and reorients myosin S1, affects the orientation of CaD* in the ternary complex. These results are consistent with a two-state binding model of caldesmon for actin in which state 1 involves a site that is competitive with S1 binding and state 2 involves a site that is formed in the presence of bound S1.

Smooth muscle contraction is primarily regulated by Ca^{2+}-calmodulin stimulation of myosin light chain phosphorylation in the thick filament. Evidence is accumulating, however, for additional regulatory mechanisms involving the thin filament-associated protein, caldesmon. Caldesmon is an elongated molecule with an N-terminal, myosin-binding region, a C-terminal region involved in actin binding and in the inhibition of ATPase, and a central, α-helical spacer region [for a review, see Sobue and Sellers 1991; Marston & Redwood, 1991; Chalovich, 1993]. Caldesmon is thought to take part in regulation by inhibition of actomyosin ATPase activity, which is reversed either by caldesmon phosphorylation or the binding of Ca^{2+}-calmodulin to caldesmon. It is not entirely clear whether ATPase inhibition is due to a reduction in myosin binding to actin (Chalovich et al., 1987; Hemric & Chalovich, 1988; Horiuchi & Chacko, 1989; Horiuchi et al., 1991; Velaz et al., 1989, 1990) or to a slowing of the rate-limiting step in the ATPase kinetic pathway (Marston & Redwood, 1992) or both (Horiuchi & Chacko, 1989). Either mechanism is consistent with the fact that caldesmon binds somewhere close to, or indirectly affects, the N-terminal (Bartegi et al., 1990; Levine et al., 1990; Adams et al., 1990) and C-terminal (Graceffa & Jancso, 1991; Crosbie et al., 1991; Kolakowski et al., 1992) regions of actin, which also contain the myosin-binding sites. To better understand the role of caldesmon in the regulation of the interaction between actin and myosin, we studied the binding of caldesmon and that of its 27-Da C-terminal fragment, labeled with the fluorescent probe acrylodan,[1] to skeletal muscle ghost myofibrils and the effect of myosin S1 on this interaction. Myofibrils provide an intact, oriented actin filament system which allows measurements of the orientation of the label on caldesmon by linear dichroism using fluorescence microscopy. We found that caldesmon and S1 can form a ternary complex with actin in which the orientation of bound caldesmon, and therefore its interaction with actin, are altered as compared to the caldesmon–actin binary complex.

MATERIALS AND METHODS

Preparations. Caldesmon from fresh chicken gizzard was purifed from the 30–50% $(NH_4)_2SO_4$ fraction of the heat-stable extract (Bretscher, 1984) by DEAE-Sephadex A-50 and phosphocellulose P-11 chromatography (Graceffa & Jancso, 1991). A 27-kDa C-terminal fragment of caldesmon (Lys 579–Pro 756) was expressed as a cII fusion protein in *Escherichia coli* and isolated as described previously (Wang et al., 1991). This fragment migrates on SDS–polyacrylamide gel with an apparent molecular weight of 27 000, although its true molecular size, deduced from its amino acid sequence, is 24 000 (Wang et al., 1991). Rabbit skeletal myosin S1 was prepared by chymotryptic cleavage of myosin (Weeds & Pope, 1977) using Mg^{2+} to selectively precipitate rod and undigested myosin (Okamoto & Sekine, 1985). Protein concentrations were determined using the following optical extinction coefficients (1 mg/mL) and molecular weights, respectively: caldesmon, $E_{280} = 0.33$, 88 000 (Graceffa et al., 1988; Bryan et al., 1990; Hayashi et al., 1989); 27-kDa C-terminal fragment of CaD, $E_{280} = 0.36$, 24 000; myosin S1, $E_{280} = 0.75$, 115 000. Muscle fibrils were prepared from rabbit psoas muscle fibers stored at −20 °C in 50% glycerol by a short treatment with

† This work was supported by (1) a Research Fellowship from the American Heart Association, Massachusetts Affiliate, Inc., to D.S., (2) National Institutes of Health Grants HL-22461 (S.S.L.), AR-30917 (P.G.), and HL-41411 and AR-41637 (C.-L.A.W.), (3) American Heart Association Grant-in-Aid 901345 (C.-L.A.W) and (4) National Science Foundation Grant DMB-8817581 (S.S.L.).

‡ Permanent address: Nencki Institute of Experimental Biology, 3 Pasteur St., 02-093 Warsaw, Poland.

® Abstract published in *Advance ACS Abstracts,* May 1, 1994.

[1] Abbreviations: acrylodan, 6-acryloyl-2-(dimethylamino)naphthalene; CaD*, acrylodan-labeled caldesmon; CaD-27*, acrylodan-labeled 27-kDa C-terminal fragment of caldesmon; S1, myosin subfragment 1; HMM, heavy meromyosin; IATR, iodoacetyltetramethylrhodamine; PMSF, phenylmethanesulfonyl fluoride; DTT, dithiothreitol; SDS, sodium dodecyl sulfate; EDTA, ethylenediaminetetraacetic acid.

0006-2960/94/0433-6716$04.50/0

a polytron homogenizer and low-speed centrifugation. After the myofibrils were washed with the rigor buffer, 0.03 M NaCl, 3 mM $MgCl_2$, 0.5 mM DTT, and 10 mM Hepes, pH 7.2, they were stored on ice in the same buffer containing 0.5 mM PMSF to prevent damage to the Z-lines by endogenous proteases. Ghost myofibrils (free of myosin, tropomyosin, and troponin), with intact actin-containing I-bands, were prepared by washing myofibrils attached to a microscope slide with Hasselbach–Schneider solution (0.5 M NaCl, 1 mM MgCl, 10 mM $NaPP_i$, 20 mM phosphate buffer, pH 6.4). After washing with rigor buffer, the attached ghost myofibrils were incubated with labeled or unlabeled actin-binding proteins as described below.

Labeling of Proteins. Labeling of caldesmon at both cysteines (Cys 153, Cys 580) and of the 27-kDa fragment at Cys 580 with acrylodan was performed in a solution containing about 0.5 mg/mL protein in 40 mM NaCl, 0.2 mM EDTA, 5 mM MOPS buffer, pH 7.5, for 2 h at room temperature with 5× molar excess of acrylodan. Myosin S1 was labeled with iodoacetyltetramethylrhodamine (IATR) by incubation of 2 mg/mL of S1 for 14 h in the dark at 0 °C with equimolar dye. The labeling reaciton was quenched by addition of 5 mM DTT and dialyzed versus rigor buffer. The molar labeling ratios of acrylodan/CaD = 2.20, acrylodan/CaD-27 = 1.04, and IATR/S1 = 0.30 were obtained using the following extinction coefficients for the fluorescent probes: ϵ_{365}(acrylodan) = 12 900 M^{-1} cm^{-1} and ϵ_{557}(IATR) = 37 000 M^{-1} cm^{-1}.

Steady-State Fluorescence Measurements. Fluorescence excitation, emission, and polarization (P) spectra of acrylodan-labeled caldesmon (CaD*) and its acrylodan-labeled 27-kDa C-terminal fragment (CaD-27*) were obtained with a Spex Fluorolog 2/2/2 photon-counting fluorometer (Spex Industries, Inc.). Spectra were obtained in the ratio mode with 2.25-nm band-pass for excitation and emission wavelengths of 365 and 500 nm, respectively. Protein concentrations were $\simeq$4 μM for CaD* and $\simeq$10 μM for CaD-27*.

Fluorescence Microscopy. Fluorescence-detected linear dichroism measurements were performed on myofibrils using a fluorescence microscope as detailed by Szczesna and Lehrer (1992) and summarized here. A suspension of myofibrils (50 μL) was placed on a microscope slide and covered with a cover slip containing 0.15-mm spacers. Myofibrils, which naturally attach to the slide, were incubated with Hasselbach–Schneider solution to remove myosin, troponin, and tropomyosin. A solution of CaD* or CaD-27* was then introduced into the microscope cell, followed by rigor buffer that contained an oxygen scavenging system (0.3% glucose, 0.16 mg/mL glucose oxidase, and 0.016 mg/mL catalase), to minimize photobleaching, and bovine serum albumin (0.5 mg/mL), to minimize nonspecific binding of added protein. Solutions of tropomyosin, S1, or IATR-labeled S1 were similarly introduced into the cell, with excess unbound protein washed out with rigor buffer. Solutions containing MgADP also contained 100 μg/mL hexokinase to remove ATP contamination.

Linearly polarized light from a 50-W mercury lamp was directed through a Zeiss dichroic mirror assembly (no. 05 for acrylodan and no. 14 for IATR) and a 100 × /1.3 NA fluorescence objective onto the selected area (three sarcomeres) of the fibril placed in a cell on a stage of a fluorescence microscope. The emitted light was collected by the objective and measured by photon couting. The angular dependence of the fluroescence (F) is given by $F = {}^1/_2 \sin^2 \Psi \sin^2 \Theta + \cos^2 \Psi \cos^2 \Theta$, where Ψ is the angle between the myofibrillar axis and the polarization direction of the excitation and Θ is the average polar angle between absorption dipole of the dye and the fibril axis. The dichroic ratio R (for excitation polarized parallel and perpendicular to the axis of the fibril) is $R = F(\Psi=0°)/F(\Psi=90°) = 2 \cot^2 \Theta$. R is therefore dependent on the average orientation of the fluorescent probe on caldesmon relative to the fibril axis. The above equation assumes no probe disorder in this system (see Results and Discussion).

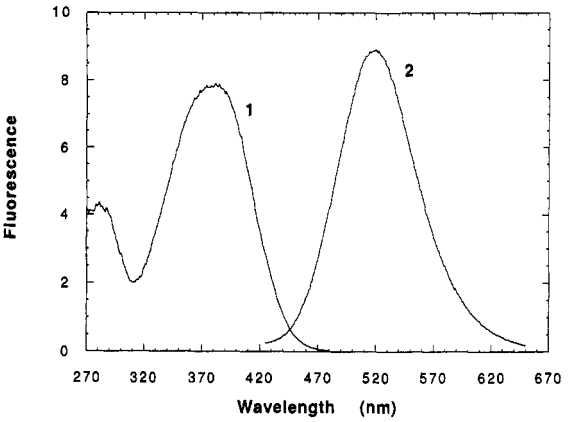

FIGURE 1: Fluorescence excitation (1) and emission (2) spectra for acrylodan-labeled caldesmon ($\simeq$4 μM) in solution containing 0.03 M NaCl, 3 mM $MgCl_2$, 0.5 mM DTT, and 10 mM Hepes, pH 7.2. Excitation and emission wavelengths were 365 and 500 nm, respectively.

RESULTS

Characterization of the Fluorescence of CaD and CaD-27*.* The emission and excitation spectra of the acrylodan probe have been shown to be sensitive to the polarity of its environment (Weber & Farris, 1979; Marriott, 1987; Rottenberg, 1992). The excitation and emission spectra of CaD* in solution (shown in Figure 1) were identical to those of CaD-27* (not shown). The emission peak at 520 nm and excitation peak at 385 nm indicate that the fluorescence arises from probes on both proteins in a similar polar environment. Since caldesmon and CaD-27* share the same probe at Cys 580, the additional probe at Cys 153 for caldesmon also appears to be located in a polar environment. To estimate the mobility of the acrylodan probe on caldesmon and on the CaD-27* fragment, the fluorescence polarization (P) excitation spectra in solution were measured. In the wavelength region excited by the microscopic dichroic filter assembly (400–440 nm), P = 0.26 and 0.33 for CaD* and CaD-27*, respectively. The relatively high degree of polarization of CaD-27*, which is expected to increase when attached to fibrils, compared to the rigid value, P = 0.4, for this probe (Szczesna & Lehrer, 1992) suggests that the probe covalently bound to Cys 580 does not significantly rotate during its lifetime and can be considered to have a fixed orientation. The smaller value for CaD* indicates that the second labeled site (Cys 153) has a higher mobility, which results in a lower average polarization value.

Dichroism Measurements. Upon irrigation of ghost myofibrils (Figure 2b) with CaD* or CaD-27* (4 μM in rigor buffer), an immediate appearance of fluorescence on the fibril was observed associated with the binding of caldesmon or the 27-kDa fragment to actin. The fluorescence was localized in the actin-containing I-bands of fibrils excluding the Z-line region (Figure 2c1). Using fluorescence-detected linear dichroism, the average orientation angle (Θ) of the fluorescent probe relative to the myofibrillar axis (see Materials and Methods) was determined. CaD*, as well as CaD-27*, bound

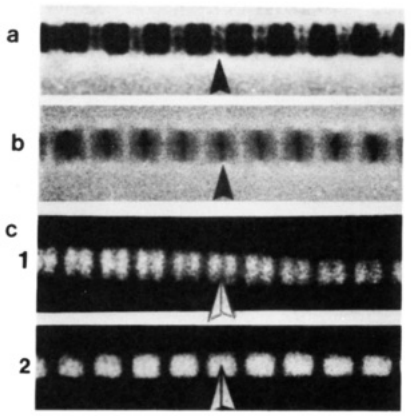

FIGURE 2: Pattern of ternary complex formation between actin, myosin S1, and caldesmon. (a) Phase-contrast photograph of intact myofibril containing A- and I-bands. Arrowheads show Z-lines. (b) Phase-contrast photograph of ghost myofibril obtained by washing an intact fibril with Hasselbach–Schneider solution. Note loss of myosin-containing A-bands, leaving actin-containing I-bands attached to Z-lines. (c) Acrylodan-labeled caldesmon bound to the actin in ghost fibril in the presence of IATR-labeled myosin S1: (1) acrylodan fluoresence of caldesmon isolated by the acrylodan (no. 05) dichroic filter assembly; (2) rhodamine fluorescence of IATR-S1 isolated by the rhodamine (no. 14) dichroic filter assembly.

Table 1: Effect of Myosin S1 on the Orientation of Acrylodan-Labeled Caldesmon (CaD*) or Acrylodan-Labeled 27-kDa Fragment (CaD-27*) Bound to Actin in Ghost Myofibrils

system		R^a	$\langle\Theta\rangle^b$ (deg)
ghost fibrils ± Tm	+ CaD*	1.04 ± 0.04	54.1 ± 0.5 (102)
	+ CaD-27*	1.18 ± 0.04	52.1 ± 0.5 (30)
+ S1	+ CaD*	0.62 ± 0.07	61.0 ± 1.3 (22)
	+ CaD-27*	0.79 ± 0.06	57.9 ± 1.0 (47)
+ S1[ADP]	+ CaD*	1.02 ± 0.05	54.5 ± 0.7 (24)
	+ CaD-27*	1.16 ± 0.06	52.7 ± 0.7 (26)

[a] R is the dichroic ratio for fluorescence parallel/perpendicular to the fibril axis. [b] $\langle\Theta\rangle$ is the calculated average polar angle; the number of determinations of different areas is indicated in parentheses.

to actin in ghost fibrils with positive dichroism ($R > 1$) corresponding to respective polar angles of 54.1° and 52.1°. The presence of tropomyosin did not alter the orientation of the fluorescent probes (Table 1).

Irrigation of the CaD*-bound fibril with buffer, which displaces the previous solution, did not decrease the observed fluorescence intensity, indicating tight binding of CaD* with the fibrils. However, irrigation with unlabeled myosin S1 (10 μM in rigor buffer) caused dissociation of CaD* from the fibril, reflected by the rapid loss of most of the fluorescence localized in the sarcomeres. When CaD* was reintroduced into the myofibrils, an immediate increase of fluorescence occurred, but no appreciable dissociation of myosin S1 was observed, as indicated by a lack of change of the phase contrast image of the S1-bound actin bands. This indicated that a ternary complex of actin, caldesmon, and S1 was formed. The dichroism of CaD* in the ternary complex showed a change of the probe orientation reflected by the change in dichroism from positive ($R > 1$) to negative values ($R < 1$), corresponding to average polar angles of 61° and 57.9° for CaD* and CaD-27*, respectively. Further addition of S1 did not dissociate the rebound CaD* or CaD-27* and did not affect the dichroic ratio values, suggesting that, in the presence of S1, caldesmon rebound to a different site on actin, no longer competitive with S1. Similar results were obtained when CaD* was added after first binding S1.

To verify the presence of myosin S1 in the ternary complex, IATR-S1 was bound to ghost fibrils before irrigation with CaD*. Uniform fluorescence from both probes (green fluorescence from acrylodan on caldesmon and red fluorescence from IATR on S1) was simultaneously observed from the same areas (Figure 2c1,2), indicating ternary complex formation between actin S1 and caldesmon. Introducing MgADP to the CaD*–actin–S1 ternary complex in the fibril changed the caldesmon orientation to a positive value, similar to that observed in the absence of S1 (Table 1). This change was not accompanied by the dissociation of myosin S1 or caldesmon from the fibril, as verified again by monitoring the fluorescence intensities originating from both probes (acrylodan and IATR). In control experiments, when the preformed S1·ADP complex was introduced to the CaD* complexed actin in the fibril, the positive dichroism value was the same, indicating that the order of addition was not important. Thus, CaD bound to actin has a different orientation in the ternary complex with S1–ADP compared to that with S1.

Effects of Disorder on Dichroism. In general, the measured dichroism value is sensitive to the probe orientational distribution due to effects of dynamic and static disorder. However, it appears that both types of disorder are minimal in this system so that the S1-induced change in dichroism is not due to a change in the probe distribution. Static disorder was assumed to be small (i) because we specifically selected highly oriented regions of fibrils for measurements aided by the intense observation of CaD* fluorescence and (ii) because of the specificity of the label on caldesmon. Effects of dynamic disorder were estimated from the relatively high values of measured solution polarization. For CaD*, $P = 0.26$ and was increased to $P = 0.34$ in the presence of actin in the excitation wavelength region used in the microscope. These values gave an estimate for the maximum angle through which the probe rotates during its lifetime (Lakowicz, 1983): 30° and 20° for CaD* and CaD*–actin, respectively. Assuming a Gaussian distribution of half-width, 15° and 10°, the effect on the measured dichroic ratio for CaD* bound to actin as a result in a change in dynamic disorder should not be greater than ±5% for $R = 1.04$ (Szczesna & Lehrer, 1992). However, the changes in R observed upon S1 binding were much greater (40%) for both CaD* and CaD-27*, showing that changes in dynamic disorder do not significantly contribute. It should be noted that the change in sign of the dichroism cannot be explained simply by a change in order.

DISCUSSION

The naturally oriented actin filaments of myofibrils provide a scaffold for the binding of labeled proteins, allowing for the determination of the orientation of labels relative to the fibril axis with measurements of fluorescence-detected linear dichroism (Borejdo et al., 1982; Szczesna & Lehrer, 1992). For a relatively immobile probe such as acrylodan on caldesmon, as shown above by the high degree of polarization, a change in the probe orientation means a change in the orientation of the protein domain to which the probe is attached.

In the absence of myosin S1, CaD* bound to actin with a probe polar angle of 54.1°, which was not affected by the presence of tropomyosin on actin. Introducing excess S1 into the fibrils resulted in the dissociation of caldesmon from actin, in agreement with studies which show that nucleotide-free S1 competes with caldesmon for actin binding (Hemric & Chalovich, 1988) considering the high affinity of S1 for actin ($K = 10^8$ M^{-1}) relative to caldesmon for actin ($K = 10^6$ M^{-1}) (Velaz et al., 1990) and the high free concentration of S1 present in the solution compared to caldesmon. However,

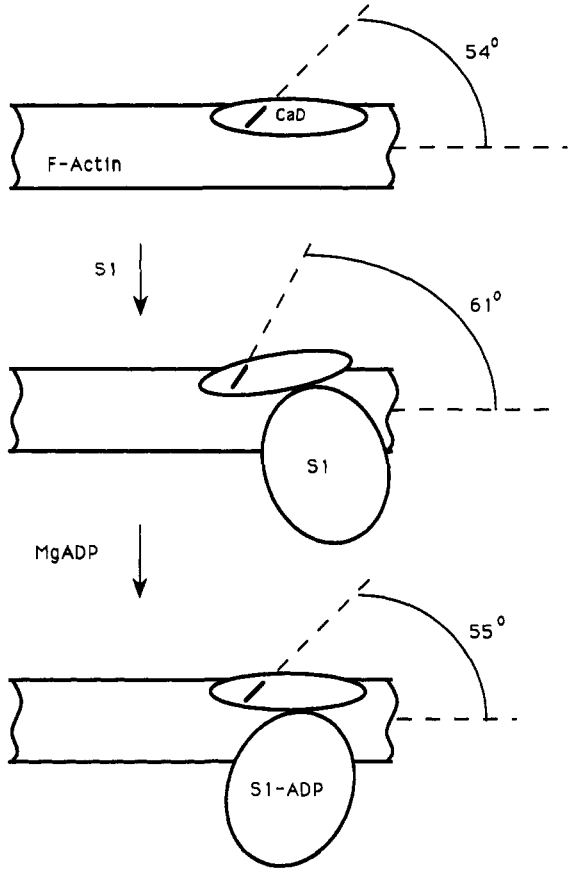

FIGURE 3: Schematic diagram of the different orientations of caldesmon on actin involved by myosin S1.

reintroduction of CaD* to fibrils saturated with S1 resulted in the rebinding of CaD*, in a ternary complex with actin–S1, with a new probe angle of 61°. A similar 6–7° change in angle was observed with C-terminal fragment CaD-27*. Evidence for a ternary complex between F-actin, S1–AMP–PNP, and caldesmon was obtained from binding studies (Chen & Chalovich, 1992) and has previously been observed in electron micrographs with S1 (Harricane et al., 1992). Our studies further indicate, however, that in the ternary complex the caldesmon molecule, or part of it, is bound to a new site (with a new orientation) on actin which appears to be occupied only in the presence of bound S1. In a preliminary experiment with intact rigor fibrils, CaD* was noted to bind to actin with a similar orientation as for the ternary complex in the ghost fibril. However, the influence of troponin on CaD and S1 binding needs to be ascertained before it can be concluded that the actin subunits need not be saturated with myosin heads to change the CaD orientation.

Interestingly, when MgADP was bound to S1 in the ternary complex, the probe orientation changed back to its original value without dissociation of S1. Binding of ADP to S1 in fibrils and fibers results in a change in orientation of S1 (Borejdo et al., 1982; Szczesna & Lehrer, 1992; Tanner et al., 1992) which presumably allows caldesmon to return to its original orientation and position on actin. Since the orientation of caldesmon is changed by a changed orientation of S1 on actin, close proximity between S1 and caldesmon is suggested. This is consistent with the fact that caldesmon and myosin S1 both bind to similar region on actin (Bartegi et al., 1990; Levine et al., 1990; Adams et al., 1990; Graceffa & Jansco, 1991).

A schematic model depicting the changes in orientation of caldesmon is shown in Figure 3. In the absence of S1, actin binds caldesmon at site 1 with a probe angle of 54°. Site 1 can bind caldesmon or S1 but not both (a competitive site). In the presence of bound S1, caldesmon can bind to site 2 with a probe angle of 61°. Site 2 can be occupied by caldesmon only in the presence of bound S1 (a conditional noncompetitive site). The competitive nature of caldesmon in site 1 agrees with caldesmon inhibition of actin-activated S1–ATPase activity in solution (Chalovich et al., 1987; Horicuchi & Chacko, 1989) and force generation in fibers (Brenner et al., 1991) and is consistent with caldesmon binding to actin with a stronger binding constant ($K_a = 10^6\ M^{-1}$) than that of S1·ATP or S1–ADP·P_i to actin ($K_a \simeq 10^3\ M^{-1}$). Presumably, caldesmon at site 2 would be in a noninhibitory state.

The extended caldesmon molecule binds to many actin subunits along the filament with the C-terminal domain interacting most strongly with a few actin subunits. However, the nature of the putative ternary complex is unclear; i.e., do both sites 1 and 2 exist on each actin subunit? A model based on actin-binding studies with caldesmon and S1–AMPPNP has been proposed whereby one or two actin subunits of the several subunits that interact with caldesmon contain only one site which can competitively bind either caldesmon or S1 and ternary complexes can be noncompetitively formed with the other actin subunits (Chen & Chalovich, 1992). Our observation that the C-terminal domain of CaD adopts a different orientation in the presence of bound S1 is not inconsistent with the Chen and Chalovich model whereby S1 affects caldesmon via ternary complex formation with neighboring subunits at the noncompetitive sites. However, S1 could also affect caldesmon orientation via ternary complex formation with the actin subunits that bind the C-terminal caldesmon domain at the conditional sites. Further studies will be needed to elucidate the nature of the ternary complex.

REFERENCES

Adams, S., DasGupta, G., Chalovich, J. M., & Reisler, E. (1990) *J. Biol. Chem. 265*, 19652–19657.
Bartegi, A., Fattoum, A., & Kassab, R. (1990) *J. Biol. Chem. 265*, 2231–2237.
Borejdo, J., Assulin, O., Ando, T., & Putnam, S. (1982) *J. Mol. Biol. 158*, 391–414.
Brenner, B., Yu, L. C., & Chalovich, J. M. (1991) *Proc. Natl. Acad. Sci. U.S.A. 88*, 5739–5743.
Bretscher, A. (1984) *J. Biol. Chem. 259*, 12873–12880.
Chalovich, J. M. (1993) *Pharmacol. Ther. 55*, 95–148.
Chen, Y., & Chalovich, J. M. (1992) *Biophys. J. 63*, 1063–1070.
Crosbie, R., Adams, S., Chalovich, J. M., & Reisler, E. (1991) *J. Biol. Chem. 266*, 20001–20006.
Graceffa, P., & Jancso, A. (1991) *J. Biol. Chem. 266*, 20305–20310.
Graceffa, P., Wang, C.-L. A., & Stafford, W. F. (1988) *J. Biol. Chem. 263*, 14196–14202.
Harricane, M. C., Bonet-Kerrache, A., Cavadore, C., & Mornet, D. (1991) *Eur. J. Biochem. 196*, 219–224.
Harricane, M. C., Fabbrizio, E., Arpin, C., & Mornet, D. (1992) *Biochem. J. 287*, 633–637.
Hemric, M. E., & Chalovich, J. M. (1988) *J. Biol. Chem. 263*, 1878–1885.
Horiuchi, K. Y., & Chacko, S. (1989) *Biochemistry 28*, 9111–9116.
Horiuchi, K. Y., Samuel, M., & Chacko, S. (1991) *Biochemistry 30*, 712–717.
Kolakowski, J., Makuch, R., & Dabrowska, R. (1992) *FEBS Lett. 309*, 65–67.
Lakowicz, J. R. (1983) in *Principles of fluorescence Spectroscopy*, pp 134–139, Plenum Press, New York.
Levine, B., Moir, A. J. G., Audemard, E., Mornet, D., Patchell, V. B., & Perry, V. (1990) *Eur. J. Biochem. 193*, 687–696.

Marriott, G. (1987) "Dynamic Aspects of Protein Structure – a Fluorescence Spectroscopic Approach", Thesis, University of Illinois, Urbana.
Marston, S. B., & Redwood, C. S. (1991) *Biochem. J. 279*, 1–16.
Marston, S. B., & Redwood, C. S. (1992) *J. Biol. Chem. 267*, 16796–16800.
Okamoto, Y., & Sekine, T. (1985) *J. Biochem. (Tokyo) 98*, 1143–1145.
Rottenberg, H. (1992) *Biochemistry 31*, 9473–9481.
Sobue, K., & Sellers, J. R. (1991) *J. Biol. Chem. 266*, 12115–12118.
Szczesna, D., & Lehrer, S. S. (1992) *Biophys. J. 61*, 993–1000.
Tanner, J. W., Thomas, D. D., & Goldman, Y. E. (1992) *J. Mol. Biol. 223*, 185–203.
Velaz, L., Hemric, M. E., Benson, C. E., & Chalovich, J. M. (1989) *J. Biol. Chem. 264*, 9602–9610.
Velaz, L., Ingraham, R. H., & Chalovich, J. M. (1990) *J. Biol. Chem. 265*, 2929–2934.
Wang, C.-L. A., Wang, L.-W. C., Xu, S., Lu, R. C., Saavedra-Alanis, V., & Bryan, J. (1991) *J. Biol. Chem. 266*, 9166–9172.
Weber, G., & Farris, F. J. (1979) *Biochemistry 18*, 3075–3078.
Weeds, A. G., & Pope, B. (1977) *J. Mol. Biol. 111*, 129–157.